Negative transconductance in double-gate germanium-on-insulator field effect transistors

A. Zaslavsky[a)]
Division of Engineering, Brown University, Providence, Rhode Island 02912, USA

S. Soliveres
IES, Université de Montpellier II, 34095 Montpellier Cedex 5, France

C. Le Royer
CEA-LETI/Minatec, 17 rue des Martyrs, 38054 Grenoble Cedex 9, France

S. Cristoloveanu
IMEP-INPG/Minatec, 3 parvis Louis Néel, 38016 Grenoble Cedex 1, France

L. Clavelier and S. Deleonibus
CEA-LETI/Minatec, 17 rue des Martyrs, 38054 Grenoble Cedex 9, France

(Received 23 July 2007; accepted 4 October 2007; published online 31 October 2007)

Transport in double-gate (DG) transistors offers unusual properties due to the coupling between the two channels. We report on room-temperature negative transconductance in germanium-on-insulator DG transistors in the subthreshold regime. The effect is due to the coupling between conducting channels, analogous to the velocity modulation transistor (VMT). Unlike the VMT, our effect can be induced by either of the gates and arises not from a difference in the channel mobilities but from partial electric field screening at low channel densities combined with the density dependence of mobility. The negative transconductance becomes weaker as gate length L_G is reduced. © *2007 American Institute of Physics*. [DOI: 10.1063/1.2802074]

Most predictions concerning the future evolution of semiconductor technology[1] invoke changes in transistor architecture from single to multiple gate and the introduction of alternative channel materials. In double-gate (DG) silicon-on-insulator (SOI) devices, the coupling between the independently controlled channels offers an additional degree of freedom.[2] Thus, asymmetric front gate (V_{FG}) and back gate (V_{BG}) gate biasing can be used to achieve symmetric electron populations in DG SOI transistors and improve the current drive,[3] as well as to investigate the differences in mobility at the top and bottom interfaces.[4]

In this letter we report on the observation of negative transconductance g in the subthreshold current-voltage characteristics of DG germanium-on-insulator (GeOI) n-channel transistors at room temperature. Over a range of V_{FG} and V_{BG} in the subthreshold regime, both $g_{FG} \equiv \partial I_D / \partial V_{FG}$ (at constant V_{BG}) and $g_{BG} \equiv \partial I_D / \partial V_{BG}$ (at constant V_{FG}) become negative in large DG transistors, with gate length $L_G = 10\ \mu$m. The negative g persists up to drain voltage $V_D \sim 200$ mV, is reproducible from device to device, does not depend on the direction of the gate sweep, and is not due to gate leakage. It can, however, be explained by the charge coupling between the front and back channels, reminiscent of the velocity modulation transistor (VMT).[5] The VMT was demonstrated in coupled III-V double-quantum wells[6] and, more recently, discussed and modeled for DG SOI devices.[7,8]

Our GeOI transistors were fabricated on an ~230 nm buried oxide, with an unintentionally doped p-Ge channel, a front oxide of ~1 nm SiO_2 followed by 4 nm of HfO_2, and a TiN gate.[9] The typical front-gate $I_D(V_{FG})$ and transconductance g_{FG} of a submicron $L_G = 0.35\ \mu$m device at $V_D = 50$ mV and $V_{BG} = 0$ (applied to the substrate) are shown in Fig. 1(a). The I_{ON}/I_{OFF} ratio is $>10^4$ and a subthreshold slope S is ~105 mV/decade, reasonable for Ge n-type MOS.[10,11] At large front-channel density, the mobility estimated from the linear low-field $I_D(V_D)$ characteristic at

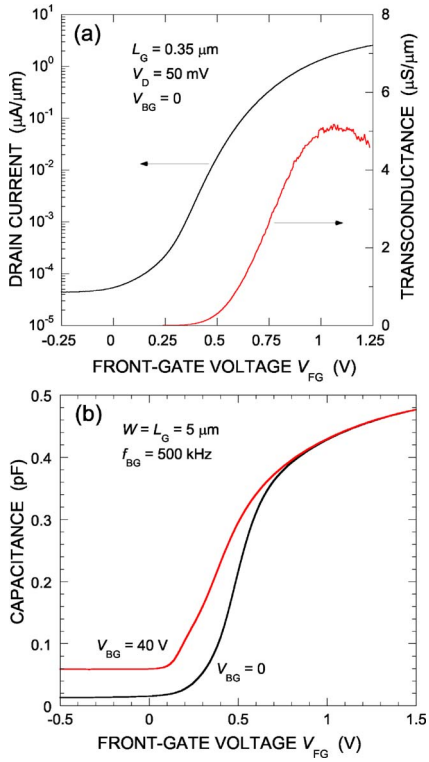

FIG. 1. (Color online) (a) Room-temperature $I_D(V_{FG})$ and transconductance characteristics of a submicron $L_G = 0.35\ \mu$m GeOI transistor at $V_D = 50$ mV and $V_{BG} = 0$. (b) High-frequency 500 kHz split-$C(V_{FG})$ data on a $W = L_G = 5$ transistor at $V_{BG} = 0$ and 40 V, permitting the extraction of gate capacitance in inversion ($V_{FG} = 1.5$ V) and the Ge channel thickness $t_{Ge} \sim 80$ nm from the differences in measured $C(V_{FG} = -0.5\ \text{V})$ at $V_{BG} = 0$ and 40 V.

[a)]Author to whom correspondence should be addressed. Electronic mail: alexander_zaslavsky@brown.edu

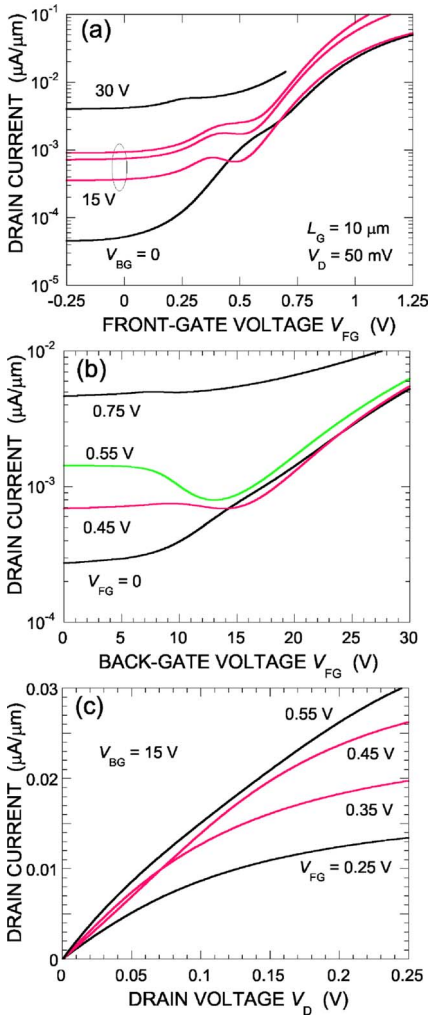

FIG. 2. (Color online) (a) Front-gate $I_D(V_{FG})$ characteristics vs V_{BG}=0, 15, and 30 V at V_D=50 mV (with added V_D=130 and 210 mV curves for V_{BG}=15 V) of a large $W=L_G=10$ μm GeOI transistor. (b) Back-gate $I_D(V_{BG})$ characteristics vs V_{FG} in the same device. (c) $I_D(V_D, V_{FG})$ curves of the same device for V_{BG}=15 V, showing the negative transconductance g_{FG} at low V_D (crossing I_D curves as V_{FG} is increased from 0.45 to 0.55 V).

V_{FG}=1.25 V and V_{BG}=0 is $\mu_{FG}\sim 11$ cm^2/V s (not corrected for series resistance). Similarly, the above-threshold back channel mobility is $\mu_{BG}\sim 16$ cm^2/V s. Figure 1(b) shows the split-$C(V_{FG})$ characteristic at f=500 kHz of a 5×5 μm^2 GeOI transistor at V_{BG}=0 and 40 V. At this f, the interface states are inactive[12] and comparing the capacitance for $V_{FG}<0$ at V_{BG}=0 and V_{BG}=40 V, we obtain a Ge layer thickness $t_{Ge}\sim 80$ nm.[13] The p-type background doping in the channel is $\sim 3\times 10^{17}$ cm^{-3}, as measured on similar GeOI substrates and consistent with the split-$C(V_{FG})$ data in Fig. 1(b).

The $I_D(V_{FG})$ curves of an L_G=10 μm transistor for several V_{BG} values at V_D=50 mV (and higher) are shown in Fig. 2(a). In the front-gate subthreshold regime, $0.3<V_{FG}<0.55$ V, the $I_D(V_{FG})$ at V_{BG}=0 displays a weak feature, which strengthens and develops into a clear region of $g_{FG}<0$ at V_{BG}=15 and 20 V, and subsequently weakens for V_{BG}=30 V. At its strongest, near V_{BG}=15 V, negative g_{FG} persists up to V_D=200 mV.

The corresponding back-gate $I_D(V_{BG})$ characteristics at V_D=50 mV for several values of V_{FG} in the same device are shown in Fig. 2(b). Again, there is a range of V_{FG} for which $g_{BG}<0$ near V_{BG}=15 V, with I_D dropping by a factor of ~ 2 in the V_{FG}=0.55 V curve. Finally, a representative set of

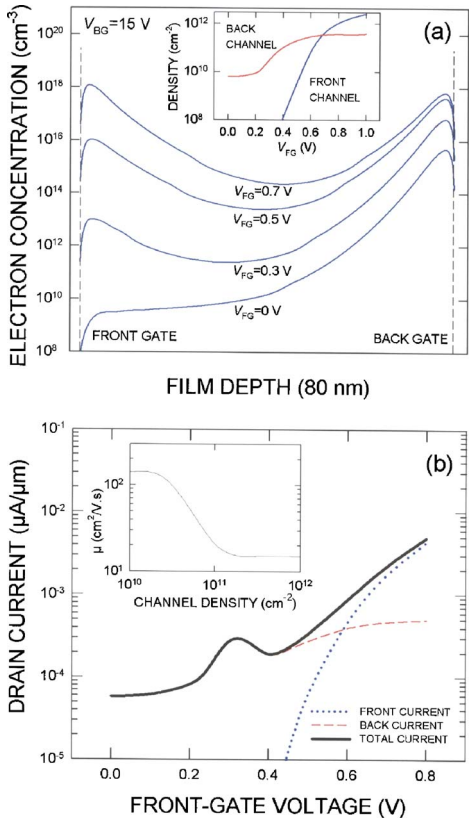

FIG. 3. (Color online) (a) Electron concentration in the Ge channel vs V_{FG} at V_{BG}=0, with integrated front and back channel densities shown in the inset. (b) Simulated subthreshold $I_D(V_{FG})$ at V_{BG}=15 V, using the mobility-density dependence shown in the inset.

$I_D(V_D, V_{FG})$ traces at V_{BG}=15 V is shown in Fig. 2(c). At sufficiently high V_D=0.3 V, g_{FG} is always positive, with higher V_{FG} resulting in higher I_D, but there exists a region of negative transconductance for $V_D<150$ mV. The channel differential resistance always remains positive: $g_D \equiv \partial I_D/\partial V_D>0$ regardless of the V_{FG} and V_{BG} biasing conditions [see Fig. 2(c)].

We attribute the observed negative subthreshold g_{FG} and g_{BG} to charge coupling between the two channels, illustrated in Fig. 3 using a self-consistent Schrödinger-Poisson numerical solution.[14] If the two channels are assumed to be in equilibrium—a reasonable assumption for low V_D and large L_G—and the channel densities are not too high, then the electric field induced by V_{FG} is not completely screened by the quasi-two-dimensional (2D) front-channel electrons[15] and can affect the back channel density and *vice versa* (this phenomenon can also be expressed in terms of threshold voltage control by the opposite gate[16]). The calculated electron density in the Ge channel with the back channel biased into weak inversion by V_{BG}=15 V and $0<V_{FG}<0.7$ V and the corresponding integrated front and back channel densities are shown in Fig. 3(a). As V_{FG} is increased, the density in the front channel increases exponentially, whereas the density in the back channel increases more slowly up to $V_{FG}\sim 0.6$ V and then saturates, see inset of Fig. 3(a). As the back channel is closer to its threshold, its contribution to I_D first increases and then drops due to the mobility degradation of μ_{BG}. At even higher V_{FG} the front channel takes over. The interplay between the channel densities thus produces the negative g_{FG}, as shown in the simulated subthreshold I_D in Fig. 3(b), obtained from an inversion charge compact model in the dif-

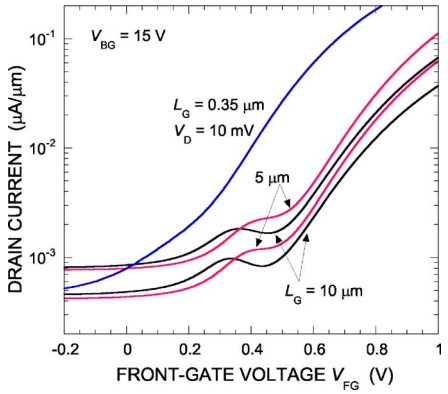

FIG. 4. (Color online) Negative front-gate transconductance feature vs gate length L_G at $V_{BG}=15$ V: the parallel vertically displaced traces correspond to $L_G=10$ and 5 μm at $V_D=50$ and 100 mV; the single line with a barely visible shoulder is the $L_G=0.35$ μm device at $V_D=10$ mV.

fusive regime. The mobility-density dependence we used is shown the inset of Fig. 3(b). We assume a low-density mobility of ~ 100 cm^2/V s (consistent with reported results on modern *n*-channel Ge transistors with thin high-κ dielectrics[10,11]), a high-density mobility of ~ 10 cm^2/V s as measured on our devices, and a crossover to the lower mobility that occurs at a lower density ($\sim 10^{11}$ cm^{-2}) than measured in Si (Ref. 17) or simulated in Ge.[18] This assumed density dependence of mobility, which drops faster than the increase in electron density in the opposite channel, is required to reproduce negative g_{FG} before the front-channel conduction takes over—the front and back channel components of subthreshold I_D are indicated in Fig. 3(b). The same mobility-density dependence explains the negative g_{BG} of Fig. 2(b). On the other hand, if a more typical mobility-density dependence with mobility decrease near mid-10^{11} cm^2/V s is assumed,[18] the simulated negative transconductance weakens into a barely visible shoulder in g at higher I_D. Clearly, the agreement with the measured $I_D(V_{FG})$ should be taken as qualitative only, as the real density dependence of our mobilities will require Hall effect measurements on DG GeOI structures, which we plan to fabricate.

It is important to distinguish our negative transconductance from the classic VMT,[5–8] where the two coupled conduction channels are designed with sharply different mobilities (e.g., Sampedro *et al.*[8] simulated an SOI VMT with a mobility ratio of 40), leading to a very sharp current drop as electrons shift from the high-mobility channel to the low-mobility one due to gate biasing. The opposite shift to the high-mobility channel in the VMT cannot lead to negative transconductance, whereas our results in Fig. 2 exhibit both negative g_{FG} and g_{BG}. Further, at least above threshold, the mobilities of our front and back channels are comparable. Our mechanism, based on incomplete screening of the electric field by low-density channels coupled with a decrease in the mobility as the channel density increases, is fully reversible if V_{FG} and V_{BG} are interchanged. The absence of hysteresis in the measured $I_D(V_{FG})$ curves and the fact that g becomes negative rules out other possible mechanisms, such as floating-body effects[19] and substrate depletion.[2]

Interestingly, the negative transconductance we observe weakens as the device gate length L_G is reduced. The comparison of $I_D(V_{FG})$ at $V_{BG}=20$ V, measured in identically processed devices with different L_G, is shown in Fig. 4: strong negative g_{FG} of the $L_G=10$ μm device is weaker in the $L_G=5$ μm, continues to weaken in $L_G=0.75$ and 0.5 μm devices (not shown), and finally survives as a barely visible shoulder in our smallest $L_G=0.35$ μm device. This is not due to changes in the V_D-induced longitudinal channel electric field, as can be verified directly by comparing the 10 and 5 μm devices at $V_D=100$ and 50 mV, respectively. We hypothesize that in submicron devices, the electron distribution in the front and back channels could be significantly different from the long-channel equilibrium conditions simulated in Fig. 3. Also, the vertical coupling between the channels in long DG devices becomes two-dimensional at small L_G. Modeling short-channel devices would require a major effort for which we lack some basic elements, such as a reliable electron mobility model.

In summary, we have observed negative transconductance in the room-temperature subthreshold characteristics of DG GeOI transistors, both as a function of front and back-gate voltages with the other gate held at a constant bias. The physical mechanism for this effect is the redistribution of charge between the two inversion channels, as in the VMT device.[5–8] However, unlike the VMT, in our devices negative transconductance can be induced both when electrons are shifted from back channel to the front (by increasing V_{FG} at fixed V_{BG}) and when they are shifted in the opposite direction. Hence it arises not from dissimilar mobilities in the two channels but from the incomplete screening of the electric field by a low-density channel combined with the density dependence of mobility in Ge inversion channels.

This work was supported by the French RTB (Basic Technology Research) and Carnot projects. A.Z. also acknowledges support by the NSF (Award No. ECCS-0701635 and DMR-0302222).

[1]The latest ITRS CMOS technology predictions are on http://public.itrs.net website
[2]G. K. Celler and S. Cristoloveanu, J. Appl. Phys. **93**, 4955 (2003).
[3]D. Esseni, M. Mastrapasqua, G. K. Celler, C. Fiegna, L. Selmi, and E. Sangiorgi, IEEE Trans. Electron Devices **50**, 802 (2003).
[4]A. Ohata, S. Cristoloveanu, and M. Casse, Appl. Phys. Lett. **89**, 032104 (2006).
[5]H. Sakaki, Jpn. J. Appl. Phys., Part 2 **21**, L381 (1982).
[6]K. J. Webb, E. B. Cohen, and M. R. Melloch, IEEE Trans. Electron Devices **48**, 2701 (2001).
[7]M. Prunnila, J. Ahopelto, K. Henttinen, and F. Gamiz, Appl. Phys. Lett. **85**, 5442 (2004).
[8]G. Sampedro, F. Gamiz, A. Godoy, M. Prunnila, and J. Ahopelto, Appl. Phys. Lett. **86**, 202115 (2005).
[9]C. Le Royer, L. Clavelier, C. Tabone, C. Deguet, L. Sanchez, J.-M. Hartmann, M.-C. Roure, H. Grampeix, and S. Deleonibus, Proc. ESSDERC, pp. 457–461 (2007).
[10]H. Shang, K. L. Lee, P. Kozlowski, C. D'Emic, I. Babich, E. Sikorski, M. Ieong, H.-S. P. Wong, and W. Haensch, IEEE Electron Device Lett. **25**, 135 (2004).
[11]W. P. Bai, N. Lu, A. Ritenour, M. L. Lee, D. A. Antoniadis, and D.-L. Kwong, IEEE Electron Device Lett. **27**, 175 (2006).
[12]A. Dimoulas, G. Vellianitis, G. Mavrou, E. K. Evangelou, and A. Sotiropoulos, Appl. Phys. Lett. **86**, 223507 (2005).
[13]J. Chen, R. Solomon, T.-Y. Chan, P.-K. Ko, and C. Hu, IEEE Electron Device Lett. **12**, 453 (1991).
[14]ATLAS User's Manual, Silvaco, 2007.
[15]S. Luryi, Appl. Phys. Lett. **52**, 501 (1988).
[16]H. K. Lim and J. G. Fossum, IEEE Trans. Electron Devices **30**, 1244 (1984).
[17]S. Takagi, A. Toriumi, M. Iwase, and H. Tango, IEEE Trans. Electron Devices **41**, 2357 (1994).
[18]T. O'Regan and M. Fischetti, J. Comput. Electron. **6**, 81 (2007).
[19]M. Bawedin, S. Cristoloveanu, G. J. Yun, and D. Flandre, Solid-State Electron. **49**, 1547 (2005).